Group-Wise Consistent Fiber Clustering Based on Multimodal Connectional and Functional Profiles

Bao Ge[1], Lei Guo[1], Tuo Zhang[1], Dajiang Zhu[2], Kaiming Li[1], Xintao Hu[1], Junwei Han[1], and Tianming Liu[2]

[1] School of Automation, Northwestern Polytechnical University, Xi'an, China
{oct.bob,guolei.npu,zhangtuo.npu,dajiang.zhu,likaiming,
xintao.hu,junweihan2010}@gmail.com
[2] Department of Computer Science, University of Georgia, Athens, GA
tliu@cs.uga.edu

Abstract. Fiber clustering is an essential step towards brain connectivity modeling and tract-based analysis of white matter integrity via diffusion tensor imaging (DTI) in many clinical neuroscience applications. A variety of methods have been developed to cluster fibers based on various types of features such as geometry, anatomy, connection, or function. However, identification of group-wise consistent fiber bundles that are harmonious across multi-modalities is rarely explored yet. This paper proposes a novel hybrid two-stage approach that incorporates connectional and functional features, and identifies group-wise consistent fiber bundles across subjects. In the first stage, based on our recently developed 358 dense and consistent cortical landmarks, we identified consistent backbone bundles with representative fibers. In the second stage, other remaining fibers are then classified into the existing backbone bundles using their correlations of resting state fMRI signals at the two ends of fibers. Our experimental results show that the proposed methods can achieve group-wise consistent fiber bundles with similar shapes and anatomic profiles, as well as strong functional coherences.

Keywords: DTI, Fiber clustering, Resting state fMRI, Fiber Classification.

1 Introduction

Automatic fiber clustering based on diffusion tensor imaging (DTI) has become a very active research area for the purpose of group-based statistical analysis on the fiber bundles [3-9]. However, DTI tractography algorithms typically generate a large number (10,000–100,000) of fibers per subject, which makes the information provided by the fibers not easily comprehensible. Therefore, the large number of fibers is often grouped into fiber bundles by fiber clustering methods [3-9] to facilitate group-wise tract-based analysis.

A typical framework is to first define a similarity between pairwise fibers and then input the similarity matrix to standard data clustering algorithms. Therefore, various similarity measures have been proposed in the literature including geometric, anatomical,

N. Ayache et al. (Eds.): MICCAI 2012, Part III, LNCS 7512, pp. 485–492, 2012.

connectional and functional characteristics of fibers [3-9]. For example, Maddah et al. [4] represented fibers as 3D quintic B-splines, Brun et al. [5] tried to capture the three geometric features using a 9-D descriptor, Corouge et al. [6] and Gerig et al. [7] proposed a mean closest distance that contains position and shape information, and Maddah et al. [3] enhances the Hausdorff similarity with Mahalanobis distance between fiber points. Later, anatomical (or atlas-based) feature was used to guide fiber clustering automatically/semi-automatically [11]. Recently, Ge et al. [8] made attempts to use the functional correlation derived from resting state fMRI (R-fMRI) data to guide fiber clustering.

This paper presents a novel two-stage hybrid fiber clustering approach that clusters fibers in a hierarchical way based on connectional and functional features. Specifically, the first stage groups a portion of fibers into group-wise consistent representative backbone bundles based on our recently developed 358 dense and consistent cortical landmarks [2]. The second stage classifies other remaining fibers into the backbone bundles obtained in the first stage according to functional coherences derived from R-fMRI data. The major advantage of this methodology is that those consistent and common 358 cortical landmarks define and form the reliable and corresponding backbone fiber bundles, which serve as the reliable reference for the following clustering of less consistent fibers. Furthermore, in the second stage, the traditional fiber clustering problem is converted into a fiber classification problem in which the functional coherence derived from R-fMRI data guides the fiber clustering procedure. In short, the proposed two-stage fiber clustering methodology effectively utilizes the deep-rooted common connectional and functional brain architectures to guide the fiber clustering processes such that the obtained fiber clusters possess both structural and functional correspondences across individuals, which was demonstrated by our experimental results.

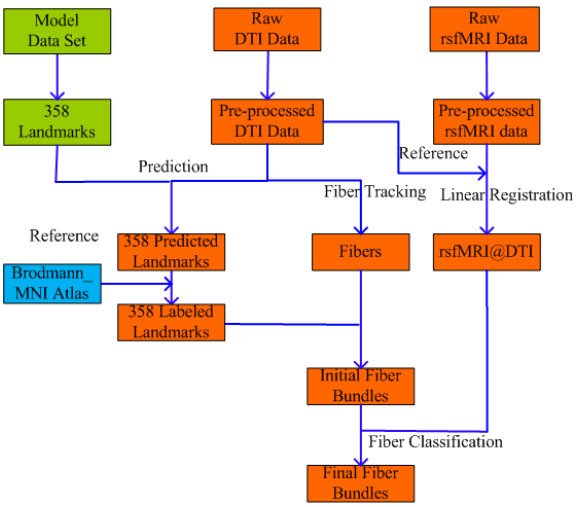

Fig. 1. Flowchart of the proposed computational framework

2 Materials and Methods

2.1 Overview

As summarized in Fig.1, our algorithmic pipeline includes the following steps. First, we pre-processed the raw DTI data and R-fMRI data, and then performed fiber tracking based on DTI data. Also, we registered the R-fMRI signals to the DTI space using FSL FLIRT. In the meantime, we predicted the 358 consistent landmarks for all subjects via the methods in [2], and grouped/labeled these 358 landmarks by the MNI (Montreal Neurological Institute) atlas. Then, we identified the backbone fiber bundles based on these consistent cortical landmarks, and each backbone bundle is represented by several representative fibers. Finally, we represented the backbone fiber bundles by the mean R-fMRI signals of these fibers, and classified other remaining fibers into these backbone bundles by comparing the wavelet-derived correlations of the R-fMRI signals.

2.2 Multimodal Data Acquisition and Pre-processing

Eight student volunteers were scanned using a 3T GE Signa MRI system under IRB approvals. We acquired the R-fMRI data with the dimensionality of 128*128*60*100, space resolution 2mm*2mm*2mm, TR 5s, TE 25ms, and flip angle 90 degrees. DTI data was acquired using the same spatial resolution as the R-fMRI data; the parameters were TR 15.5s and TE 89.5ms, with 30 DWI gradient directions and 3 B0 volumes acquired. Pre-processing of the R-fMRI data included brain skull removal, motion correction, spatial smoothing, temporal pre-whitening, slice time correction, global drift removal, and band pass filtering (0.01Hz~0.1Hz). For the DTI data, pre-processing steps included brain skull removal, motion correction, and eddy current correction. After the pre-processing, fiber tracking was performed using MEDINRIA (FA threshold: 0.2; minimum fiber length: 20). The DTI image space was used as the standard space from which to generate the tissue segmentation map and from which to show the functionally coherent fiber bundles on the cortical surface. DTI and fMRI images were registered via FSL FLIRT.

2.3 Identifying Backbone Fiber Bundles via 358 Consistent Cortical Landmarks

Recently, we identified and validated 358 group-wise consistent cortical landmarks that possess intrinsic correspondences across individuals and populations [2]. These landmarks have consistent DTI-derived fiber connection patterns and exhibit corresponding functional locations. Importantly, they have been reproduced in over 240 individual brains [2]. Thus, these 358 landmarks offer a universal and individuated brain reference system. In particular, these 358 landmarks can be accurately predicted in each individual brain with DTI data [2]. Figure 2(a) shows an example of these 358 landmarks.

Based on the MNI atlas, first, we grouped these landmarks into Brodmann-labeled classes, 37 Brodmann areas were used to label the 358 landmarks. We performed this step on one randomly chosen subject once, and then these labeled landmarks can be

applicable to other subjects because the 358 cortical landmarks possess correspondences. Figure 2(b) shows the MNI-labeled landmarks with different colors. Then, the backbone fiber bundles were identified base on the landmarks' labels that the fiber's two ends connect. That is, we grouped all of fibers connecting the same two Brodmann labels into the same backbone fiber bundle, thus we found the 32 common backbone bundles across 8 subjects by finding the common Brodmann labels across subjects. Quantitatively, these fibers count for approximately 6%~12% of all fibers in the whole brains of different subjects. Fig. 2(c) shows an example of backbone bundles.

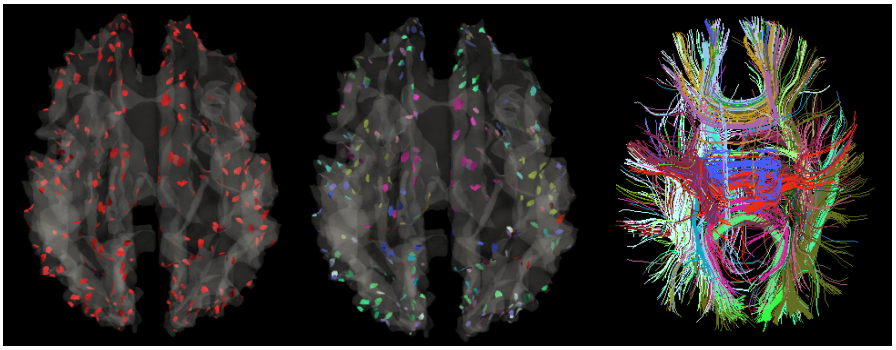

(a) (b) (c)

Fig. 2. (a) 358 landmarks (in red) from one randomly chosen subject. (b) The grouped/labeled landmarks via the MNI atlas. Each color represents one Brodmann area. (c) The grouped backbone fiber bundles. Each color represents one backbone bundle. The colors have no correspondences with those in (b).

2.4 Fiber Classification via Functional Coherence

The above identified backbone fiber bundles possess intrinsic correspondences across different brains because of the existing correspondences established by the 358 cortical landmarks [2]. Then, they are used as the common and reliable reference for the second stage of fiber clustering through fiber classification. The basic idea is that the remaining fibers are classified to one of the backbone bundles based on the Wavelet-based functional coherence derived from R-fMRI data.

Wavelet analysis is particularly well suited for the analysis of cortical fMRI time series in the resting state [13]. Specifically, the maximal overlap discrete wavelet transform (MODWT) is a redundant transform that is translation invariant and easy to compute using the pyramid algorithm. In particular, it does not suffer from the DWT's sensitivity to the choice of a starting point for a time series, and thus is adopted in this paper.

The steps of using MODWT for fiber classification are described as follows.

1. First, we extracted the R-fMRI signal from gray matter voxels that the fiber's two end points connect, using the method similar to [8]. One fiber has two time series signals, which were denoted by X_{i1}, X_{i2}, and the average value is X_i.

2. Then, the mean R-fMRI signal (X_{jmean}) within each backbone fiber bundle was computed. That is, $X_{jmean} = mean(X_i)$ for the *jth* bundle.
3. The MODWT was used to decompose each mean fMRI time series into the following scales or frequency intervals [10]: scale 1, 0.16–0.31 Hz; scale 2, 0.08–0.16 Hz; scale 3, 0.04–0.08 Hz; and scale 4, 0.02–0.04 Hz. Afterwards, we computed the MODWT wavelet coefficients ($\widetilde{W}_{j=3}^{X}$) on scale 3 of the wavelet decomposition.
4. For each other remaining fiber that is neighboring to the fibers within the backbone bundle, we computed the MODWT wavelet coefficients ($\widetilde{W}_{j=3}^{Y}$) in the same manner. Also, the wavelet correlation [1] between the fiber and each backbone fiber bundle was then computed as $|\rho_{XY}|$, and the fiber was classified into the backbone fiber bundle with maximal correlation value, which must be larger than a predefined threshold in order to ensure that the most relevant fibers are selected.

Notably, in this work, we focused on the scale 3 of the wavelet decomposition in that this is the frequency band most commonly studied in R-fMRI analyses and represents a reasonable trade-off between avoiding the physiological noise associated with higher frequency oscillations and the measurement error associated with estimating very low frequency correlations from limited time series [10]. And the threshold was chosen empirically. We manually selected the 11 fiber bundles according to the method in [12], and computed the functional correlation values between fibers within each bundle, then averaged them for all 11 fiber bundles. The averaged value of 0.7 was chosen as threshold.

3 Experimental Results

In total, we identified 32 group-wise consistent fiber bundles for the whole brain, as shown in Fig 3. For the purpose of visual differentiation, each fiber bundle was represented by the representative fiber (shown in Fig 3(b)) whose mean closest distance with other fibers within the bundle was minimal. Each corresponding fiber bundle and the representative fiber in Fig. 3 have the same color in different brains. It is evident that the distributions of these 32 representative fibers are quite reasonable and consistent. As a more detailed example, Fig.4 shows 8 consistent fiber bundles from two randomly selected subjects. For a quantitative comparison, we computed the Hausdorff distances between the corresponding representative fibers of the eight subjects, as shown in Table 1. It can be seen that the Hausdorff distances are relatively small.

Moreover, we compared the percentages of streamline fibers in the 8 backbone fiber bundles and those of the corresponding finally clustered bundles after the second stage classification in Table 2. On average, the percentage of consistently clustered fibers increases from 8.03% to 25.78%, suggesting that the group-wise consistent backbone fiber bundles can really serve as the common white matter fiber tracts for clustering, and not all fibers were clustered into these 32 bundles because the 358 landmarks can only cover a portion of the cortex. Table 3 shows the functional coherence of the 8 final fiber bundles with the corresponding backbone fiber bundles. We can see that final fiber bundles maintain the high functional coherence after classification. These above results demonstrated the fiber bundles have both similar connection patterns and functional coherences.

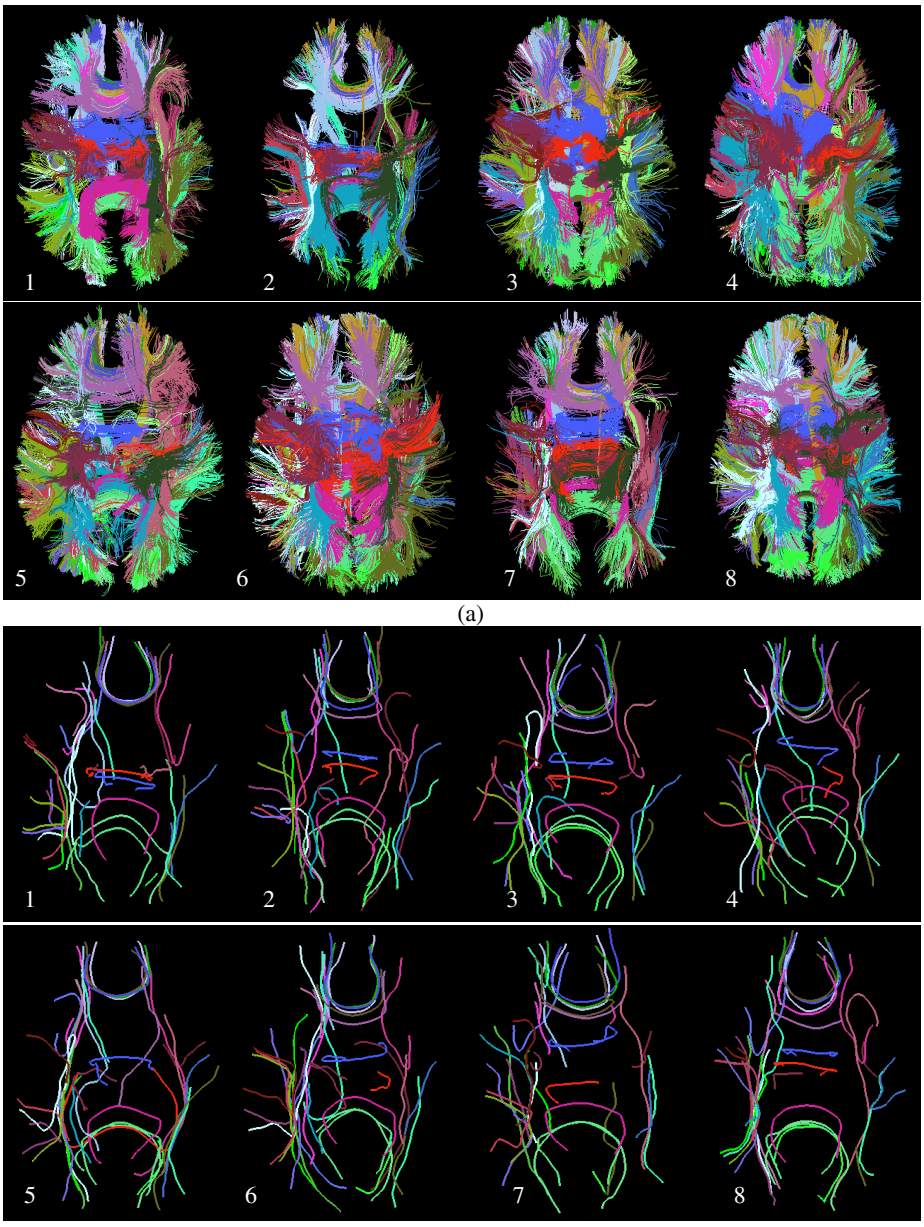

Fig. 3. The 32 group-wise consistent fiber bundles for 8 subjects. (a) The 32 fiber bundles with the corresponding colors across subjects. (b) The 32 representative fibers of bundles for each subject with the same corresponding colors as in (a).

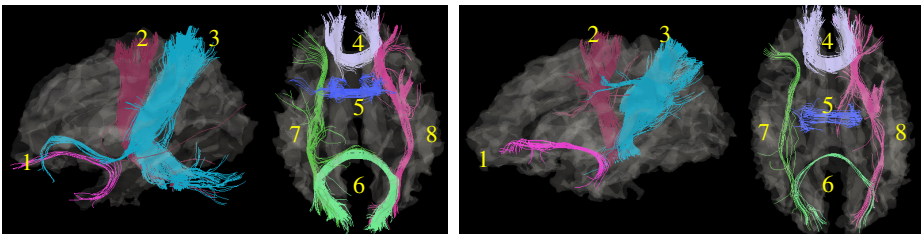

(a) (b)

Fig. 4. The detailed visualization of 8 consistent fiber bundles from 2 subjects (a) and (b). The same corresponding fiber bundle (indexed by numbers) is in the same color.

Table 1. Hausdorff distances (mm) between the 8 consistent corresponding fiber bundles across 8 subjects

	$Dis_{s1,s2}$	$Dis_{s1,s3}$	$Dis_{s1,s4}$	$Dis_{s1,s5}$	$Dis_{s1,s6}$	$Dis_{s1,s7}$	$Dis_{s1,s8}$
1	2.790	4.648	3.121	5.070	4.035	3.459	2.161
2	3.347	4.668	6.256	4.655	4.192	4.068	5.264
3	5.877	4.934	4.226	5.637	6.300	3.822	4.804
4	3.301	5.264	3.041	3.827	2.556	2.747	2.443
5	3.469	3.386	4.191	2.590	4.026	1.903	4.330
6	2.193	2.616	4.698	2.807	2.397	2.398	5.395
7	6.951	5.178	6.874	5.326	6.091	3.268	6.192
8	5.289	2.804	6.938	5.666	7.673	6.708	6.057

Table 2. The mean percentages of the 8 backbone fiber bundles (row #2) among all fibers in the whole brain, and those of the finally clustered fiber bundles (row #3). The total number of all the backbone fibers for all subjects is also shown (column #10).

	1	2	3	4	5	6	7	8	all
Initial	0.18%	0.72%	0.57%	0.18%	0.22%	0.14%	0.08%	0.10%	8.03%
Final	0.22%	2.06%	1.90%	1.01%	0.92%	0.35%	0.27%	0.30%	25.78%

Table 3. Functional coherence of the 8 final fiber bundles. The functional coherence was computed as the mean correlation of each fiber's R-fMRI signal (X_i) within the final fiber bundles and the mean R-fMRI signal (X_{jmean}) within each backbone fiber bundle.

	1	2	3	4	5	6	7	8
coherence	0.8065	0.7283	0.7538	0.9038	0.8347	0.8034	0.7573	0.7303

4 Conclusion

This paper proposed a new fiber clustering method that achieves group-wise consistent fiber bundles in two stages. Conceptually, this methodology utilizes the common structural and functional brain architectures inferred from DTI and R-fMRI data. In particular, the 358 cortical landmarks provide a basis for the extraction of backbone

fiber bundles, whose correspondences and consistencies are achieved automatically. In the second stage, the functional coherences derived from R-fMRI data were used to guide the classification of the remaining fibers into the already consistent backbone bundles. Both qualitative and quantitative analyses demonstrated the good performance of the proposed framework. In the future, we plan to investigate finer scale clustering of these fibers into a more structurally and functionally homogenous bundles. In addition, we plan to perform large scale task-based fMRI studies to validate the functional correspondences of these backbone fiber bundles.

References

1. Percival, D.B., Walden, A.T.: Wavelet methods for time series analysis. Cambridge UP, Cambridge (2000)
2. Zhu, D., et al.: DICCCOL: Dense Individualized and Common Connectivity-based Cortical Landmarks. Cerebral Cortex (accepted, 2012)
3. Maddah, M., Grimson, W., Warfield, S., Wells, W.: A unified framework for clustering and quantitative analysis of white matter fiber tracts. Med. Image Anal. 12(2), 191–202 (2008)
4. Maddah, M., Grimson, W., Warfield, S.: Statistical Modeling and EM Clustering of White Matter Fiber Tracts. In: ISBI, vol. 1, pp. 53–56 (2006)
5. Brun, A., Knutsson, H., Park, H.-J., Shenton, M.E., Westin, C.-F.: Clustering Fiber Traces Using Normalized Cuts. In: Barillot, C., Haynor, D.R., Hellier, P. (eds.) MICCAI 2004. LNCS, vol. 3216, pp. 368–375. Springer, Heidelberg (2004)
6. Corouge, I., Gouttard, S., Gerig, G.: Towards a Shape Model of White Matter Fiber Bundles Using Diffusion Tensor MRI. In: ISBI, pp. 344–347 (2004)
7. Gerig, G., Gouttard, S., Corouge, I.: Analysis of Brain White Matter via Fiber Tract Modeling. In: IEEE EMBS, vol. 2, pp. 4421–4424 (2004)
8. Ge, B., Guo, L., Lv, J., Hu, X., Han, J., Zhang, T., Liu, T.: Resting State fMRI-Guided Fiber Clustering. In: Fichtinger, G., Martel, A., Peters, T. (eds.) MICCAI 2011, Part II. LNCS, vol. 6892, pp. 149–156. Springer, Heidelberg (2011)
9. Ge, B., Guo, L., Li, K., Li, H., Faraco, C., Zhao, Q., Miller, S., Liu, T.: Automatic Clustering of White Matter Fibers via Symbolic Sequence Analysis. In: SPIE Medical Image, vol. 7623, pp. 762327.1–762327.8 (2010)
10. Fornito, A., Zalesky, A., Bullmore, E.: Network Scaling Effects in Graph Analytic Studies of Human Resting-State fMRI Data. Front. Syst. Neurosci. 4, 22 (2010)
11. O'Donnell, L.J., Westin, C.-F.: Automatic tractography segmentation using a high-dimensional white matter atlas. IEEE Transactions on Medical Imaging 26(11), 1562–1575 (2007)
12. Wakana, S., et al.: Reproducibility of quantitative tractography methods applied to cerebral white matter. NeuroImage 36(3), 630–644 (2007)
13. Maxim, V., Sendur, L., Fadili, M.J., Suckling, J., Gould, R., Howard, R., Bullmore, E.T.: Fractional Gaussian noise, functional MRI and Alzheimer's disease. NeuroImage 25, 141–158 (2005)